Juniper Online
Journal Material Science
ISSN: 2575-856X

Research Article
Volume 6 Issue 5 - January 2022
DOI: 10.19080/JOJMS.2022.06.555697

JOJ Material Sci
Copyright © All rights are reserved by G Bagliuk

Structure and Properties of TiCrFeNiC High Entropy Alloy Produced by Powder Metallurgy

G Bagliuk*, M Marich and A Mamonova

Institute for problems of materials science NAS of Ukraine, Ukraine

Submitted: November 14, 2021; **Published:** January 11, 2022

***Corresponding author:** G Bagliuk, Institute for problems of materials science NAS of Ukraine, Kyiv, Ukraine

Abstract

The equiatomic high entropy TiCrFeNiC alloy was prepared by sintering or hot forging of preforms from the initial or milled powder mixtures. It is shown that sintering does not provide close to non-porous state of the sintered material. The porosity of the sintered at 1300°C samples from the initial mixture is ≈ 5%, and from milled one ≈ 9%. Minimization of porosity samples (up to 1-1.5 %) was reached only at use of hot forging of porous preforms. Sintered and hot forged alloys consist of predominant high-entropy FCC phase. Dispersed inclusion of titanium carbide particles and a small content of chromium carbide Cr_3C_2 evenly distributed in matrix phase. The hot-forged alloy has a fairly high compressive strength, reaching 2250 MPa, and a hardness of 62 HRC. The annealing after hot forging and increasing of its temperature leads to a monotonic decrease in the level of strength and hardness. Annealing as well increases the level of crack resistance of the alloy, which reaches the value of 14.3 MPa×м$^{1/2}$.

Keywords: High entropy alloy; Powder metallurgy; Sintering; Hot forging; Porosity; Phase; Lattice; Carbide; Strength; Hardness; Solid solution

Introduction

In the past decade, solid solution alloys containing five or more principal elements in equi-atomic or nearly equi-atomic proportions have received considerable interest from the scientific community, which have been referred to as high entropy alloys (HEAs) [1-6].

A feature of this class of materials is the unique combination of physical and mechanical characteristics both at room and at elevated temperatures. It is believed that high mechanical properties of HEAs are provided mainly due to the fact that the presence of dissimilar atoms of elements with different electronic structures, size and thermodynamic properties in the crystal lattice of the solid solution of substitution leads to its significant distortion and slow diffusion of atoms in a multicomponent elemental matrix. This contributes to significant solid solution hardening and thermodynamic stability of properties, provides increased thermal stability of the phase composition and structural state, and, consequently, high alloy properties - hardness, strength, wear resistance, oxidation resistance, etc. The high entropy of mixing elements in the alloys causes the Gibbs free energy to be minimized and leads to the predominant formation of solid solutions with BCC, FCC or FCC + BCC structure. The phases formed on the basis of solid solutions are more stable than intermetallic compounds or other complex ordered structures [1,2].

Technologically, the most widely used methods of HEAs manufacturing are based mainly on the use of arc smelting and casting technologies [7-12]. However, alloys made by casting methods had many structural defects such as voids, porosity, dendritic liquation, etc. caused by thermal expansion and crystallization of melts. Furthermore, the cast process was complex and it was difficult to control the microstructure and performance of high entropy alloys [13]. The disadvantages inherent in casting technologies contributed to the development of powder metallurgy methods which has shown high potential as a way to manufacture HEAs [14]. Technology of powder metallurgy allows significant compositional accuracy, can completely avoid segregation, achieve superior microstructural control (including the formation of nanocrystalline materials) and easily produce metal matrix composites [14].

The possibility of using powder metallurgy methods to produce high-entropy alloys is shown in more than 250 publications concerning the manufacturing of more than 160 various alloy compositions [13-29]. The most commonly used elements of HEAs compositions are Fe, Ni, Cr and Co as base elements due to

their high mutual solubility. Among the wide variety of different powder alloys' compositions based on this elements, FeNiCrCoAl [13,15,18-20], FeNiCrCoMn [21-25] and FeNiCrCoTi [26-29] attract the closest attention of researchers.

It is noteworthy that the overwhelming majority of HEAs contain such rather expensive and scarce element as Co in quantities, which significantly narrows the economic feasibility of their widespread practical application. This makes it expedient to develop new component compositions of alloys on the basis of less costly resource-saving approaches using relatively cheap and affordable components with high enough level of basic physical and mechanical properties as to compare to high-entropy alloys obtained using more expensive alloys source components. On the other hand, carbon is one of the cheapest and most readily available chemical elements contributing to a significant increase in the mechanical properties of many alloys. Carbon has significant effects on the phase constitution and properties of the matrix alloy through interstitial strengthening, the increase of stacking fault energy, the formation of second phase and the contribution to grain refinement. Therefore, it is expected that the development of interstitial HEAs will open a promising way to obtaining promoted mechanical properties [30,31].

The positive effect of carbon on the properties of high-entropy alloys has been noted in some publications [30-33]. Nonetheless, the effects of carbon on the formation of structure and properties of HEAs have not been studied systematically and it need further investigations. A significant effect on the structure and properties of powder HEAs has the route of their manufacturing. The most common processing route to obtain products from powders is the 'press and sintering' route, which is the most extensively used route in mass production for conventional PM. However, for the most of HEAs compositions this method does not provide a density close to a pore-free state or requires rather high temperatures and continuance of sintering. This, in turn, contributes to excessive grain growth that deteriorates the mechanical properties of sintered alloys. In many papers, the route followed to obtain the bulk material from HEAs is SPS [14,20,21,26-29]. One of the main advantages of SPS is that the sintering temperature is reached rapidly, and the dwell time is usually short. Those conditions enable fully densifying the sintered material but avoiding excessive grain growth. Other methods that also combine pressure and temperature (such as other hot pressing (HP) methods or hot isostatic pressing (HIP) methods) can also attain full density, but these methods usually need higher temperatures and longer times, so grain growth is not fully avoided, and the mechanical properties can be affected [14].

On the other hand, there is practically no information on the possibility of using hot forging technology to obtain HEAs, which has shown its high efficiency in manufacturing products from a number of different powder materials [34-37]. Therefore, this present study is focused on the results of appraisal of capabilities of obtaining cobalt-free HEAs with high enough level of basic physical and mechanical properties from relatively cheap and affordable components based on the Ti-Cr-Fe-Ni-C system using hot forging technology and investigations of the structural features phase composition and mechanical properties of the obtained materials.

Materials and Experimental Details

Commercially available Ti, Cr, Fe, Ni and graphite powders were used as raw materials. The purity of all the raw elemental metal is above 99.5 %. The fractional composition of the used powders obtained using a Malvern Mastersizer 2000 laser diffraction analyzer is shown in Figure 1. Using HSC Chemistry 5.11 computer program, the mass content of each element in the mixtures was determined based on their equiatomicity (Table 1).

Table 1: The chemical compositions of the experimental powder mixture.

	Elements Content, %				
	Ti	Cr	Fe	Ni	C
Atomic content	20	20	20	20	20
Weight content	21,2	23,0	24,7	25,9	5,3

The initial mixtures were prepared by milling in a planetary mill at a weight ratio of the powders mixture to the milling body of 1:10. The rotation speed of the mill drums was 800 rpm, the milling time was 60 min. In order to prevent oxidation and segregation of powder particles, this process was carried out in an ethanol medium. The resulting mixture was compacted into cylindrical billets with a diameter of 40 mm and a height of ~15 mm with pressure of consolidation of 700 MPa. Sintering of the obtained compacts was carried out in a vacuum induction furnace. The isothermal holding time during sintering was 1 hour. Some of the consolidated preforms were hot forged in a semi-closed die (Figure 2) using 1600 kN arc-stator mechanical press. After hot forging the preforms were annealed in a shaft furnace in argon at temperatures of 1200, 1250 and 1300°C. Annealing time is 2 hours.

How to cite this article: G Bagliuk, M Marich, A Mamonova. Structure and Properties of TiCrFeNiC High Entropy Alloy Produced by Powder Metallurgy. JOJ Material Sci. 2022; 6(5): 555697. DOI: 10.19080/JOJMS.2022.06.555697

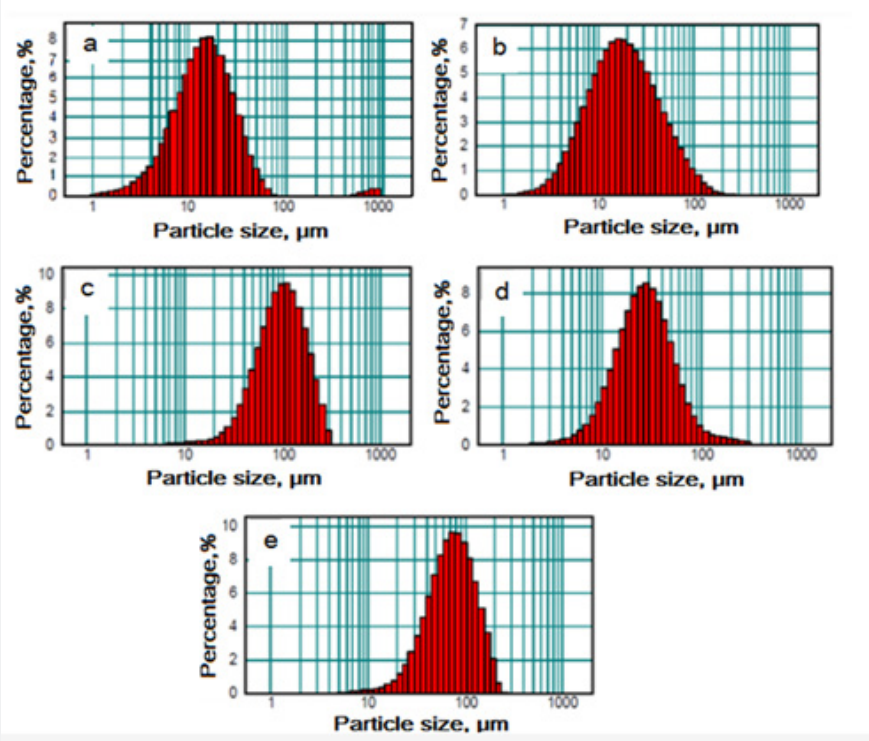

Figure 1: The fractional composition of the used powders: a - graphite; b - Cr; c - Fe; d - Ni; e - Ti.

The density and porosity of the obtained alloys were determined by the method of hydrostatic weighing. The microstructure of the alloys was studied on an XJL-17 optical microscope and on a JEOL Superprobe 733 scanning electron microscope. X-ray analysis of the samples was carried out on a DRON-3M diffractometer in filtered Co-K_{α} radiation by step-by-step scanning in the angle range 20-130°. The sample rotated around its axis during diffraction. Quantitative X-ray local microanalysis was performed using CAMECA MS-46 X-ray microscope with a microprobe spot diameter of 3μm.

The Results of the Experiments and their Discussion

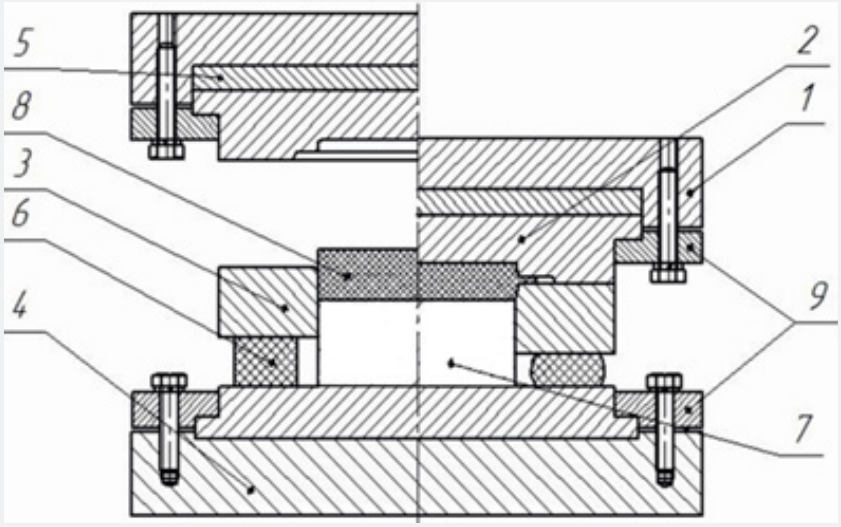

Figure 2: Experimental die for hot forging: 1 - top plate; 2 - upper semi-matrix; 3 - lower semi-matrix; 4 - lower base plate; 5 - support plate; 6 - elastic element; 7 - lower punch; 8 - forged preform; 9 - upper and lower mounting flanges.

How to cite this article: G Bagliuk, M Marich, A Mamonova. Structure and Properties of TiCrFeNiC High Entropy Alloy Produced by Powder Metallurgy. JOJ Material Sci. 2022; 6(5): 555697. DOI: 10.19080/JOJMS.2022.06.555697

As it is seen from Figure 3a, the initial mixture consists of powder particles with a morphology close to equiaxed or spherical shape. After milling the morphology of the mixture changes significantly: the powder particles acquire mainly substantially lamellar or flaky shape (Figure 3b). As a result of milling of powder mixture in a planetary mill, its dispersion noticeably increases and the fractional composition shifts towards the fine and ultrafine fractions (Figure 4).

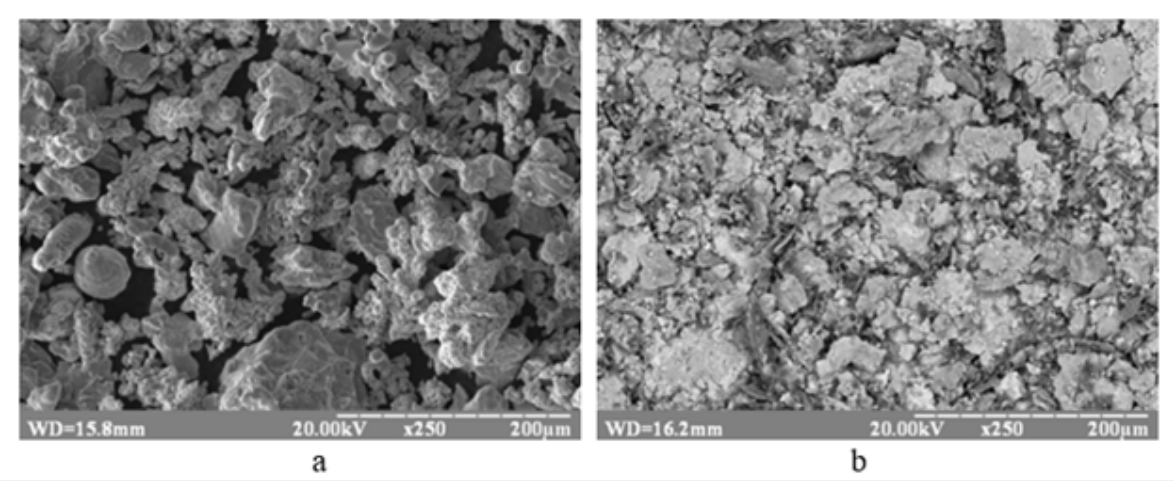

Figure 3: SEM images of the Ti-Cr-Ni-Fe-C powder mixtures: a - the initial state; b - after milling for 60 minutes.

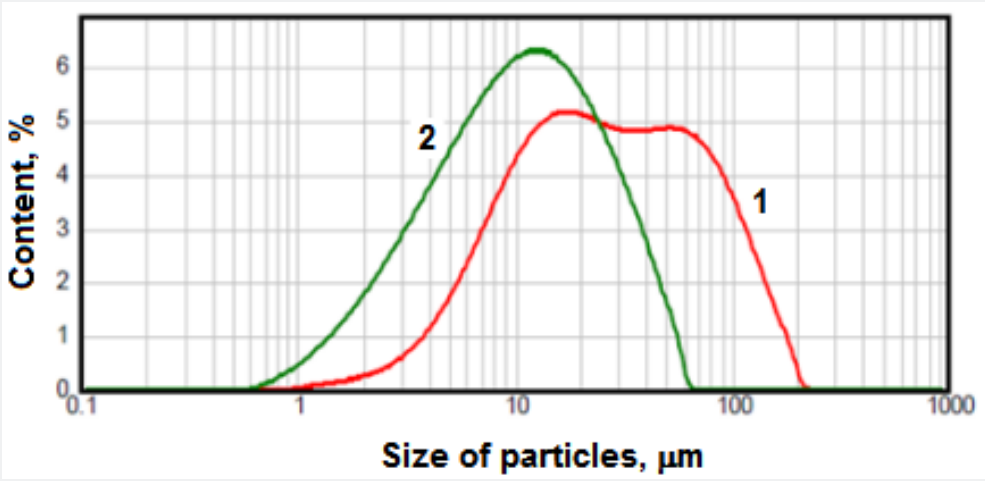

Figure 4: Fractional composition of the mixture: 1 - initial mixture; 2 - after milling for 60 minutes.

Analysis of the X-ray spectrum of TiCrFeNiC mixture after milling in a planetary mill for 60 min showed (Figure 5) that it consists of the reflexes of the individual components of the developed mixture. Therefore, chemical interaction between the components does not occur, but the nature of the reflexes profile of the alloy components changes dramatically. Significant expansion of the reflexes indicates the distortion of the crystal lattice of elements, overlapping of X-ray reflections of elements having close angles of reflection, eliminates the possibility of profile selection for calculating the parameters of the fine structure. Defects in the crystal structure intensify sintering processes and greatly affect the peculiarities of the formation of phase composition. The use of mechanoactivation significantly increases the reaction surface of the powders, significant distortion of their crystal structure and accelerates the process of alloying during further heat treatment and must have a positive effect on properties of alloys. Significant changes in the morphology of powder particles after milling led to a noticeable decrease in the bulk density of the powder mixture (up to 1.7 g/c m^3) compared to the same mixture in the initial state (2.15 g/cm^3). Changes in powders morphology as well as their work hardening in the process of high-energy milling significantly influenced the compatibility of the powder at its

How to cite this article: G Bagliuk, M Marich, A Mamonova. Structure and Properties of TiCrFeNiC High Entropy Alloy Produced by Powder Metallurgy. JOJ Material Sci. 2022; 6(5): 555697. DOI: 10.19080/JOJMS.2022.06.555697

consolidation too. Thus, the samples from the initial (unmilled) mixture after consolidation at 700 MPa had a density of 5.91 g/cm^3 (corresponding to the level of porosity of 11%), while the density of the samples consolidated from the milled mixture was only 4.62 g/cm^3 (porosity ≈ 30%) (Figure 6).

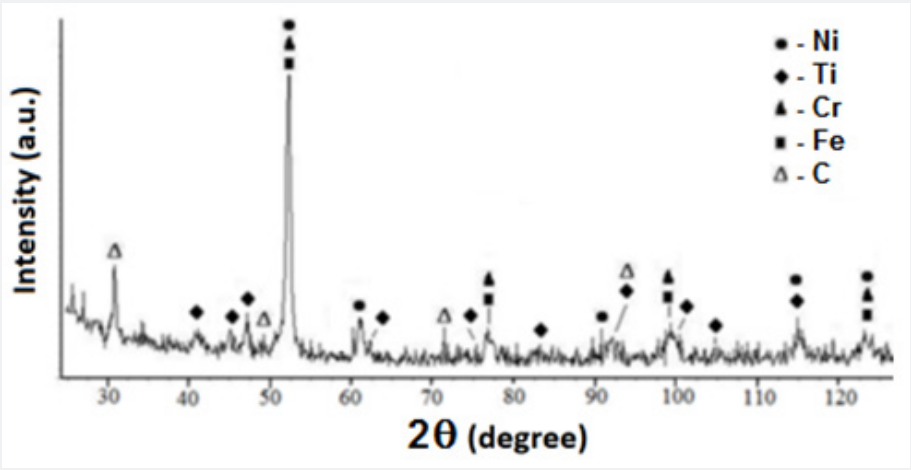

Figure 5: XRD pattern of equiatomic TiCrFeNiC powder mixture after milling for 60 min in a planetary mill.

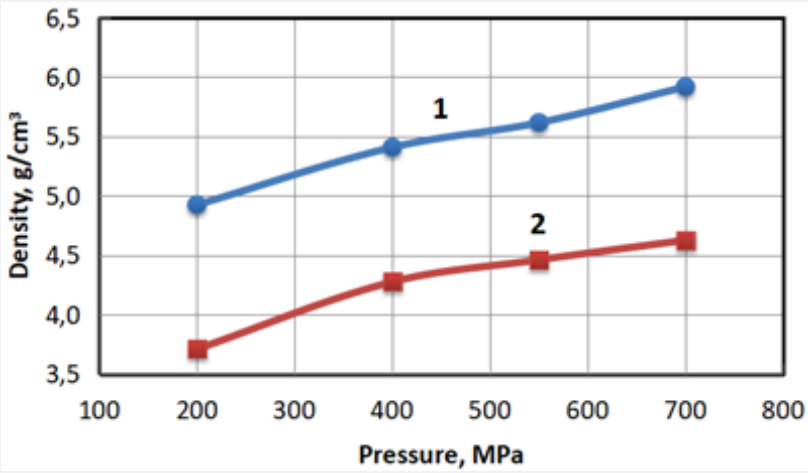

Figure 6: The compactibility of the: 1 - initial mixture (without milling); 2 - the mixture after milling.

Sintering of the samples consolidated at 700 MPa showed that at temperatures of 1100-1150°C minimal shrinkage was manifested. Only when the sintering temperature reaches the level of 1200°C sintering was activated (Figure 7) apparently due to the appearance of the liquid phase in the Fe-Ti system [38], which was observed at the sintering of powder mixtures including iron, titanium and carbon [39]. The liquid phase formed in the volume of the workpiece facilitates the development of adhesion forces between the individual powder particles, which significantly intensifies the diffusion processes and sintering in general.

In this case, the shrinkage of the samples obtained from the milled powders is greater compared to the samples, made from unmilled powders. The reason for the better shrinkage of samples from milled powders can be explained both by their higher initial porosity and due to the high level of activation of powder particles due to their intense plastic deformation during milling, which significantly increases the value of the diffusion coefficient of the components of the powder mixture.

It is noteworthy that despite the noticeable shrinkage of the samples obtained from both the original and milled mixtures, sintering temperatures even up to 1300°C do not provide a close to non-porous state of the sintered material. The porosity of the sintered at 1300°C samples made from the initial mixture is ≈ 5 %, and from the milled one ≈ 9%. The structure of the sintered alloy is

How to cite this article: G Bagliuk, M Marich, A Mamonova. Structure and Properties of TiCrFeNiC High Entropy Alloy Produced by Powder Metallurgy. JOJ Material Sci. 2022; 6(5): 555697. DOI: 10.19080/JOJMS.2022.06.555697

a gray matrix phase with evenly distributed dispersed inclusions of TiC and Cr_3C_2 carbides (Figure 8). Taking into account that for both types of powder mixtures after sintering it was not possible to obtain close to non-porous alloys, minimization of samples porosity (up to 1-1.5 %) was achieved only by using hot forging of porous preforms from mixtures of both types. Fig. 8 shows the initial preforms (Figure 9a) and the samples after their hot forging in a semi-closed die (Figure 9b).

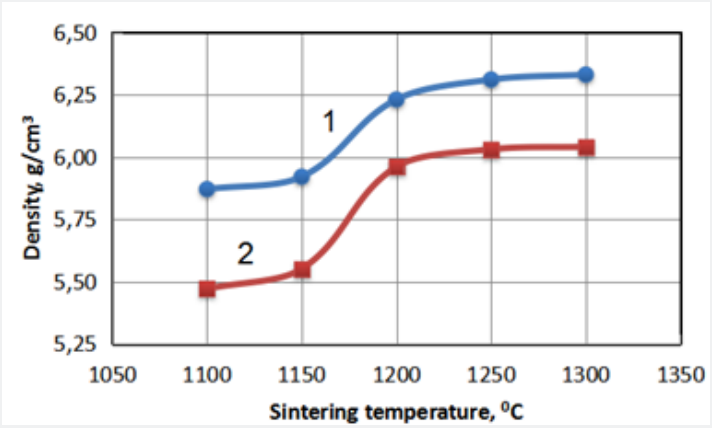

Figure 7: The effect of sintering temperature on density of sintered billets made from the initial mixture (1) (without milling) and the mixture after milling (2).

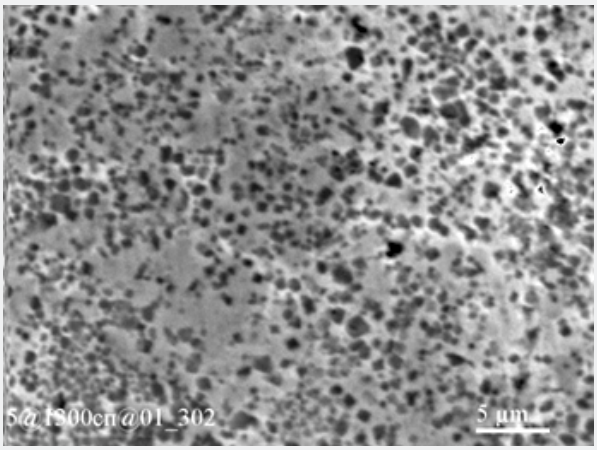

Figure 8: Microstructure of sintered at 1300oC TiCrFeNiC alloy.

Figure 9: Initial preforms (a) and hot forged samples (b).

How to cite this article: G Bagliuk, M Marich, A Mamonova. Structure and Properties of TiCrFeNiC High Entropy Alloy Produced by Powder Metallurgy. JOJ Material Sci. 2022; 6(5): 555697. DOI: 10.19080/JOJMS.2022.06.555697

Preliminary mechanical activation of the powder mixture had almost no effect on the porosity of the materials after forging. However, after annealing of hot-forged samples at 1000 – 1250°C there is some increase in porosity (up to 2 - 2.5 %) due to the Frenkel effect, which is manifested in the formation during sintering of secondary porosity due to differences in mutual heterodiffusion coefficients. The microstructure of the hot-forged TiCrFeNiC alloy (Figure 10a), as well as the alloy after hot forging and annealing at 1200 and 1250°C (Figure 10b & 10c) differs by significant anisotropy. The layers with a thickness of 1 - 5μm are placed evenly in the direction perpendicular to the direction of forging. The nature of the alloy microstructure after annealing at 1300°C differs significantly from the previous ones. The structure of the material becomes almost isotropic and consists of a matrix phase with evenly distributed inclusions of the carbide phase, which is represented by rounded inclusions with a diameter of 1-5μm (Figure 10d). This fundamental change in the nature of the structure is due to recrystallization after sintering at a temperature above the solidus point of the alloy, which is confirmed by the results of differential thermal analysis. According to the data shown in Figure 11, it is established that the solidus temperature of the alloy (beginning of melting) is 1290°C, liquidus (end of melting) - 1346°C.

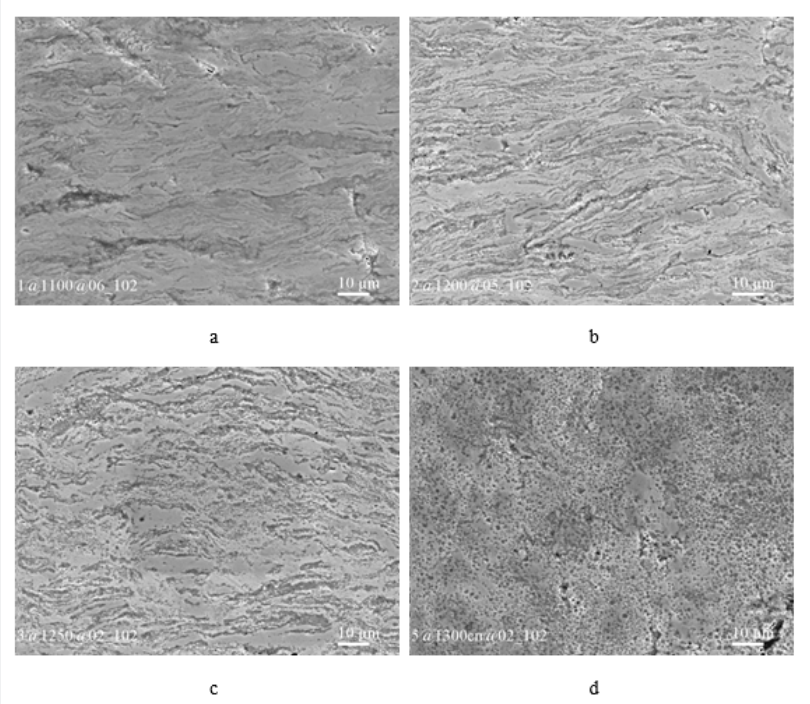

Figure 10: Microstructure of equiatomic alloys TiCrFeNiC after: hot forging (a); hot forging and annealing at 1200 (b), 1250 (c) and 1300oC (d).

The results of the X-ray diffraction (XRD) analysis of the produced material showed that the X-ray spectrum of the sintered alloy is represented mainly by FCC lines, intense titanium carbide lines with FCC lattice and weak Cr_3C_2 chromium carbide lines with orthorhombic lattice (Figure 12). The unit cell parameter of the FCC phase of the sintered alloy a = 0.35864 nm, which can be compared with the parameter of the nickel lattice, which is 0.3517nm. A significant increase in the lattice parameter of the solid-soluble phase based on the FCC structure indicates a significant distortion of the crystal lattice due to the presence of elements with different atomic radii. The line profiles are expanded, which also characterizes the distortion of the FCC lattice phase and confirmed by the numerical values of the parameters of the fine structure (Table 2).

Table 2: Parameters of fine structure of TiCrFeNiC alloys, produced by different technologies of manufacturing.

Technology of Manufacturing	α, nm	β_{111} mrad	β_{311} mrad	CSR, nm	ρ, ⍰10^{12} cm^{-2}	ε = Δ α / α, ×10^{-2}
Sintering	0,35864	7,37	21,13	24	8,94	20,72
Hot forging	0,35821	7,37	21,79	24	9,49	21,11
Hot forging + annealing 1200°C	0,35842	5,7	18,32	31,6	7,8	16,57
Hot forging + annealing 1250°C	0,35812	5,3	18,32	33,7	6,7	14,57
Hot forging + annealing 1300°C	0,3597	6,8	17,76	25,8	5,24	17,39

How to cite this article: G Bagliuk, M Marich, A Mamonova. Structure and Properties of TiCrFeNiC High Entropy Alloy Produced by Powder Metallurgy. JOJ Material Sci. 2022; 6(5): 555697. DOI: 10.19080/JOJMS.2022.06.555697

Table 2 shows the parameters of the fine structure of the TiCrFeNiC alloys, produced using different technological modes. As can be seen from the table, the use of hot forging increased the defect of the crystal lattice of the solid solution based on the phase with the structure of the FCC in comparison with the sintered alloy. The dislocation density increased from 8,94·1012 cm^{-2} for the sintered alloy to 9,49·1012 cm^{-2} for the hot-forged one. A similar pattern is manifested for the values of the micro-curvature of the lattice ($\varepsilon = \Delta a/a$) ($20.72 \cdot 10^{-2}$ and $21.11 \cdot 10^{-2}$ respectively).

In the process of high temperature annealing after hot forging at 1200 and 1250°C, annihilation of dislocations and rearrangement of the dislocation structure takes place. The defect of the crystal lattice of the main phase is markedly reduced, there is a significant decrease in the density of dislocations and micro-curvature of the lattice. The reduction of the lattice defect is also confirmed by the reduction of the expansion parameters of the lines β_{111} and β_{311}. At the same time, there is a marked increase in the size of the coherent scattering region (CSR), which characterizes the size of crystallites in metals (up to 31.6 and 33.7nm compared to 24nm for sintered and hot-forged samples). With an increase in the annealing temperature to 1300°C, the nature of the change in the parameters of the fine structure of the alloy changes somewhat. Along with a marked decrease in the dislocation's density, there is a significant decrease in the CSR parameter and an increase in the micro-curvature of the lattice. The FCC lattice parameter (0.3597nm) is also significantly increased compared to similar parameters in all other technological modes. These effects are obviously associated with a significant structural rearrangement of the alloy at the annealing temperature of 1300°C (Figure 10d), which exceeds the solidus temperature and is accompanied by further recrystallization.

When evaluating the phase composition of materials produced by sintering and hot forging, a number of factors were taken into account, which primarily include the electronic concentration of the alloy (VEC), determined by Vegard's law (mixture rule) [40]:

where c_i is the concentration of the i-th element in the alloy, x_i is its electron concentration.

The authors [21] believe that at VEC up to 4.25 el/at in the alloys a solid solution is formed on the basis of hexagonal close packed (HSP) lattice. If the average electron concentration is in the range of 4.25 - 7.2 el/at in the alloys will be formed only BCC solid solution or several solid solutions based on BCC lattice. In the transition zone from 7.3 to 8.3 el/at, the formation of two-phase solid solutions based on BCC and FCC lattice in different proportions is observed. And only at VEC ≥ 8.4 el/at a solid solution is formed on the basis of FCC lattice. The calculation of the VEC value for the TiCrFeNiC alloy showed that it is 6.4 el/at, which according to [41] should lead to the formation of a single-phase alloy based on the BCC solid solution. However, the X-ray spectrum of both sintered and hot-forged alloy is represented mainly by the FCC lines of the structural component, while the BCC lines of the structural component on the X-ray spectrum of the alloy are not explicitly detected.

The non-conformity of the phase composition of the produced alloy with the basic regularities described in [41] can obviously be caused by the redistribution of substitution elements (mainly titanium and chromium) into the carbide components. This leads to a change (increase) in the level of electronic concentration of the matrix phase, which causes the formation of two-phase (BCC and FCC) or single-phase FCC alloy. The main mechanical characteristics of alloys after hot forging and subsequent annealing at temperatures of 1200, 1250 and 1300°C are shown at Figure 13. As can be seen from the figures, the hot-forged alloy has a fairly high compressive strength, reaching 2250MPa, and a hardness of 62 HRC. High strength and high hardness characteristics are due to the solid-soluble hardening mechanism, as well as the presence of a significant content of carbide phases. At the same time, due to the high content of carbide component in the alloy, as well as mainly the FCC structure of the matrix phase, the hot-forged alloy has a low level of ductility (1%) and relatively low crack resistance (10 $MPa \times m^{1/2}$).

The use of annealing after hot forging and increasing its temperature leads to monotonic decrease in the level of strength and hardness, although even after annealing at 1300°C their level remains quite high (sy = 1266 MPa, smax = 1551 MPa, HRC 50) (Figure 12a &12b). At the same time, annealing can significantly increase the level of crack resistance of the alloy, which reaches after annealing at 1300°C the value of 14,3 $MPa \times м^{1/2}$ (Figure 13c).

Comparison of the main mechanical characteristics of hot-forged TiCrFeNiC high entropy alloy with HEAs, which contain significant amounts of expensive and scarce elements as Co, W, Hf, Ta, and Nb [1-12], showed that the alloy obtained in this work is significantly superior in strength to most HEAs obtained by using of melting and casting technologies and is at the level of the best alloys obtained by powder metallurgy methods [14]. At the same time, due to the significant amount of carbide component in the alloy, its plasticity is noticeably inferior to that of most PM HEAs of a similar class.

The nature of the fracture of hot-forged samples of TiCrFeNiC alloy is mainly transcrystallite, although the fractograms show a small number of open grain boundaries, which indicates a certain percentage of intercrystalline fracture, which characterizes the beginnings of plastic deformation (Figure 14a). After annealing and with increasing annealing temperature, the percentage of intergranular fracture increases (Figure 14b & 14c), the plasticity of the alloy increases slightly to 1.7%.

Conclusion

A significant change in the morphology of particles after milling led to a noticeable decrease in the bulk density and compactibility

How to cite this article: G Bagliuk, M Marich, A Mamonova. Structure and Properties of TiCrFeNiC High Entropy Alloy Produced by Powder Metallurgy. JOJ Material Sci. 2022; 6(5): 555697. DOI: 10.19080/JOJMS.2022.06.555697

of the powder mixture at its consolidation compared to the same mixture in the initial state. After sintering of consolidated samples at temperatures of 1100-1150 0C minimal shrinkage is manifested. Only when the sintering temperature reaches the level of 1200 0C sintering is activated apparently due to the appearance of the liquid phase in the Fe-Ti system.

Sintering do not provide a close to non-porous state of the sintered material. Minimization of samples porosity (up to 1÷1,5 %) was reached only at use of hot forging of porous preforms. X-ray spectrum of the sintered alloy is represented mainly by FCC lines, intense titanium carbide lines with FCC lattice and weak Cr_3C_2 chromium carbide lines with orthorhombic lattice. The hot-forged alloy has a fairly high compressive strength, reaching 2250 MPa, and a hardness of 62 HRC. High strength and high hardness characteristics are explained by the solid-soluble hardening mechanism, as well as the presence of a significant content of carbide phases.

The use of annealing after hot forging and increasing its temperature leads to a monotonic decrease in the level of strength and hardness, although even after annealing at 1300°C their level remains quite high (sy = 1266 MPa, smax = 1551 MPa, HRC 50). Annealing significantly increases the level of crack resistance of the alloy, which reaches after annealing at 1300 0C the value of 14,3 MPa×м$^{1/2}$.

References

1. Ranganathan S (2003) Alloyed pleasures: Multimetallic coctails. Current Science 85(10): 1404-1406.
2. Yeh JW, Chen LY, Lin SJ, Chen KS (2007) High - Entropy Alloys - A New Era of Exploitation. Materials Science Forum 560: 1-9.
3. Yeh JW (2006) Recent progress in high-entropy alloys. Ann Chim Sci Mat 31: 633-648.
4. Zhang Y, Zuo TT, Tang Z, Gao MC, Dahmen KA, et al. (2014) Microstructures and properties of high-entropy alloys. Prog Mater Sci 61(8): 1-93.
5. Dreval LA, Agraval PG, Turchanin MA (2014) High-entropy alloys as materials having a set of basic elements in the base. Bulletin of the Donbass State Machinery and Equipment Academy 1(32): 58-64.
6. Pickering EJ, Jones NG (2016) High-entropy alloys: a critical assessment of their founding principles and future prospects. Int Mater Rev 61(3): 183-202.
7. Zhang KB, Fu ZY, Zhang JY, Wang WM, Wang H, et al. (2009) Microstructure and mechanical properties of CoCrFeNiTiAl$_x$ high-entropy alloys. Mater Sci Eng A 508(1-2): 214-219.
8. CW Tsai, Chen YL, Tsai MH, Yeh JW, Shun TT, et al. (2009) Deformation and annealing behaviors of high-entropy alloy Al0.5CoCrCuFeNi. Alloys Comp 486(1-2): 427-435.
9. Wang FJ, Zhang Y (2008) Effect of Co addition on crystal structure and mechanical properties of Ti0.5CrFeNiAlCo high entropy alloy. Mater Sci Eng A 496(1-2): 214-216.
10. Zhou YJ, Zhang Y, Kim TN, Chen GL (2008) Microstructure characterizations and strengthening mechanism of multi-principal component AlCoCrFeNiTi0.5 solid solution alloy with excellent mechanical properties. Mater Lett 62(17-18): 2673-2676.
11. Tung CC, Yeh JW, Shun TT, Chen SK, Huang YS, et al. (2007) Microstructure and Characterization of Mechanically Alloyed Equiatomic AlCuCrFeMnW High Entropy Alloy. Mater Lett 61: 1-5.
12. Cantor B, Chang ITH, Knight P, Vincent AJB (2004) Microstructural development in equiatomic multicomponent alloys. Mater Sci Eng A pp. 213-218.
13. Qiu XW (2013) Microstructure and properties of AlCrFeNiCoCu high entropy alloy prepared by powder metallurgy. Journal of Alloys and Compounds 555: 246-249.
14. Torralba JM, Alvaredo P, Andrea GJ (2019) High-entropy alloys fabricated via powder metallurgy. A critical review. Powder Metallurgy 62(2): 84-114.
15. Yuhu F, Yunpeng Z, Hongyan G (2013) AlNiCrFexMo0.2CoCu high entropy alloys prepared by powder metallurgy. Rare Met Mater Eng 42(6) 1127–1129.
16. Marych M, Bagliuk G, Mamonova A, Gripachevskii A (2019) The influence of synthesis conditions on the phase composition, structure, and properties of the high-entropy Ti–Cr–Fe–Ni–Cu alloy. Powder Metallurgy and Metal Ceramics 57(9-10): 533- 541.
17. Marych M, Mamonova A, Bagliuk G (2019) Influence of the synthesis method on the crystalline structure, phase composition and properties of TiCrFeNiCuC equiatomic alloys. Materials science. Non-equilibrium phase transformations 5(1): 23-25.
18. Zhang K, Zh F, Zhang J, Wang W, Wang H, et al. (2009) Characterization of nanocrystalline CoCrFeNiCuAl high-entropy alloy powder processed by mechanical alloying. Mater Sci Forum 620-622.
19. Fan YH, Zhang YP, Guan HG, Suo HM, He L (2013) AlNiCrFexMo0.2CoCu High Entropy Alloys Prepared by Powder Metallurgy. Rare Metal Materials and Engineering 42(6): 1127-1129.
20. Fang S, Chen W, Fu Z (2014) Microstructure and mechanical properties of twinned $Al_{0.5}CrFeNiCo_{0.3}C_{0.2}$ high entropy alloy processed by mechanical alloying and spark plasma sintering. Mater Des 54: 973-979.
21. Ji W, Wang W, Wang H, Zhang J, Wang Y, et al. (2015) Alloying behavior and novel properties of CoCrFeNiMn high-entropy alloy fabricated by mechanical alloying and spark plasma sintering. Intermetallics 56: 24-27.
22. Wang B, Fu A, Huang X, Liu B, Liu Y, et al. (2016) Mechanical properties and microstructure of the CoCrFeMnNi high entropy alloy under high strain rate compression. J Mater Eng Perform 25: 2985-2992.
23. Liu B, Wang J, Liu Y, Fang Q, Wu Y, et al. (2016) Microstructure and mechanical properties of equimolar FeCoCrNi high entropy alloy prepared via powder extrusion. Intermetallics 75: 25-30.
24. Wang J, Liu Y, Liu B, Wang Y, Cao Y, et al. (2017) Flow behavior and microstructures of powder metallurgical CrFeCoNiMo0.2 high entropy alloy during high temperature deformation. Mater Sci Eng A 689: 233-242.
25. Eißmann N, Klöden B, Weißgärber T, Kieback B (2017) High entropy alloy CoCrFeMnNi produced by powder metallurgy. Powder Metall 60(3): 184-197.
26. Shaofeng Y, Yan Z, Jialin C (2014) Microstructure and properties of Al0.4FeCrNiCo1.5Ti0.3 high entropy alloy prepared by MA-HP technique. Rare Met Mater Eng 43(12): 2948-2952.
27. Moravcik I, Cizek J, Zapletal J, Kovacova Z, Vesely J, et al. (2017) Microstructure and mechanical properties of $Ni_{1,5}Co_{1,5}CrFeTi_{0,5}$ high entropy alloy fabricated by mechanical alloying and spark plasma sintering. Mater Des 119: 141-150.

How to cite this article: G Bagliuk, M Marich, A Mamonova. Structure and Properties of TiCrFeNiC High Entropy Alloy Produced by Powder Metallurgy. JOJ Material Sci. 2022; 6(5): 555697. DOI: 10.19080/JOJMS.2022.06.555697

28. Chen Z, Chen W, Wu B, Cao X, Liu L, et al. (2015) Effects of Co and Ti on microstructure and mechanical behavior of $Al_{0.75}FeNiCrCo$ high entropy alloy prepared by mechanical alloying and spark plasma sintering. Mater Sci Eng A 648: 217-224.

29. Fu Z, Chen W, Xiao H, Zhou L, Zhu D, et al. (2013) Fabrication and properties of nanocrystalline $Co_{0.5}FeNiCrTi_{0.5}$ high entropy alloy by MA-SPS technique. Mater Des 44: 535-539.

30. Guo L, Ou X, Ni S, Liu Y, Song MM (2019) Effects of carbon on the microstructures and mechanical properties of FeCoCrNiMn high entropy alloys. Materials Science & Engineering A 746: 356-362.

31. Wang Z, Baker I, Cai Z, Chen S, Poplawsky JD, et al. (2016) The effect of interstitial carbon on the mechanical properties and dislocation substructure evolution in $Fe_{40.4}Ni_{11.3}Mn_{34.8}Al_{7.5}Cr_6$ high entropy alloys. Acta Mater 120: 228-239.

32. Stepanov ND, Shaysultanov DG, Chernichenko RS, Yurchenko NY, Zherebtsov SV, et al. (2017) Effect of thermomechanical processing on microstructure and mechanical properties of the carbon-containing CoCrFeNiMn high entropy alloy. J Alloy Compd 693: 394-405.

33. Wang Z, Baker I, Guo W, Poplawsky JD (2017) The effect of carbon on the microstructures, mechanical properties, and deformation mechanisms of thermo-mechanically treated $Fe_{40.4}Ni_{11.3}Mn_{34.8}Al_{7.5}Cr_6$ high entropy alloys. Acta Mater 126: 346-360.

34. Qiu JW, Liu Y, Liu B, Liu YB (2012) Optimizing the hot-forging process parameters for connecting rods made of PM titanium alloy. Journal of Materials Science 47: 3837-3848.

35. Narayanasamy R, Senthilkumar V, Pandey KS (2006) Some aspects on hot forging features of P/M sintered iron preforms under various stress state conditions. Mechanics of Materials 38: 367-386.

36. Bagliuk G, Marich M, Mamonova A, Shishkina Y, Molchanovska G, et al. (2021) High-entropy alloy of Fe-Ti-Cr-Mn-Si-C system, produced by hot forging from powder mixtures of ferroalloys. Machines Technologies Materials 15(5): 198-200.

37. Buckingham RC, Argyrakis C, Hardy MC, Birosca S (2016) The effect of strain distribution on microstructural developments during forging in a newly developed nickel base superalloy. Materials Science & Engineering A 654: 317-328.

38. Massalski TB, Okamoto H, Subramanian PR, Kacprzak L (1996) Binary Alloy Phase Diagrams. ASM International.

39. Bagliuk G, Maksimova G, Mamonova A, Goncharuk D (2020) The Structure and Phase Composition Acquired by Fe-Ti-Ni-C Alloys in Thermal Synthesis. Powder Metallurgy and Metal Ceramics 59: 171-178.

40. Vegard L (1921) The constitution of the mixed crystals and the filling of space of the atoms. Zeitschrift fur Physik 5(1): 17-26.

41. Firstov SA, Gorban VF, Krapivka NA, Karpets MV, Pechkovskii ÉP (2016) Effect of Electron Density on Phase Composition of High-Entropy Equiatomic Alloys. Powder Metallurgy and Metal Ceramics 54: 607-613.

This work is licensed under Creative Commons Attribution 4.0 License
DOI: 10.19080/JOJMS.2020.06.555697

Your next submission with JuniperPublishers will reach you the below assets

- Quality Editorial service
- Swift Peer Review
- Reprints availability
- E-prints Service
- Manuscript Podcast for convenient understanding
- Global attainment for your research
- Manuscript accessibility in different formats
  (Pdf, E-pub, Full Text, Audio)
- Unceasing customer service

Track the below URL for one-step submission
https://juniperpublishers.com/submit-manuscript.php

How to cite this article: G Bagliuk, M Marich, A Mamonova. Structure and Properties of TiCrFeNiC High Entropy Alloy Produced by Powder Metallurgy. JOJ Material Sci. 2022; 6(5): 555697. DOI: 10.19080/JOJMS.2022.06.555697